ADVANCED MATERIALS

ring overnight at room temperature, monomer and initiator were readily absorbed in the vesicle bilayer. Photoinitiated polymerizations were performed in a thermostatted quartz reactor using either an UV-lamp (HPR 125 W, Philips) or a pulsed excimer laser (Lambda Physics XeF, 351 nm, 2 Hz pulse frequency, 30 mJ energy per pulse) as irradiation source. Conversions were determined by HPLC analysis of the residual monomers.

Details concerning the use of cryo-electron microscopy have been described earlier [19].

Received: September 15, 1999
Final version: November 10, 1999

[1] M. Antonietti, C. Göltner, A*ngew. Chem. Int. Ed. Engl.* **1997**, *36*, 991.
[2] W. Meier, *Curr. Opin. Colloid Interface Sci.* **1999**, *4*, 6.
[3] J. Hotz, W. Meier, *Adv. Mater.* **1998**, *10*, 1387.
[4] J. Murtagh, J. K. Thomas, *Faraday Discuss. Chem. Soc.* **1986**, *81*, 127.
[5] J. Kurja, R. J. M. Nolte, I. A. Maxwell, A. L. German, *Polymer* **1993**, *34*, 2045.
[6] N. Poulain, E. Nakache, A. Pina, G. J. Levesque, *Polym. Sci. Polym. Chem.* **1996**, *34*, 729.
[7] J. D. Morgan, C. A. Johnson, E. W. Kaler, *Langmuir* **1997**, *13*, 6447.
[8] J. Hotz, W. Meier, *Langmuir* **1998**, *14*, 1031.
[9] M. Jung, D. H. W. Hubert, P. H. H. Bomans, P. M. Frederik, J. Meuldijk, A. M. van Herk, H. Fischer, A. L. German, *Langmuir* **1997**, *13*, 6877.
[10] D. H. W. Hubert, P. A. Cirkel, M. Jung, G. J. M. Koper, J. Meuldijk, A. L. German, *Langmuir*, in press.
[11] M. Jung, D. H. W. Hubert, E. van Veldhoven, P. M. Frederik, A. M. van Herk, A. L. German, *Langmuir*, in press.
[12] The water solubility at 50 °C of BMA is 2.5 mM, of styrene 4.3 mM. See R. G. Gilbert, *Emulsion Polymerization: A Mechanistic Approach*, Academic, London **1995**.
[13] The propagation rate coefficients of BMA and styrene at 60 °C differ by a factor of ~3: k_p(BMA) = 1108 L mol^{-1} s^{-1} and k_p(styrene) = 341 L mol^{-1} s^{-1} , see A. M. van Herk *J.M.S.—Rev. Macromol. Chem. Phys.* **1997**, *C37*, 633.
[14] D. H. W. Hubert, *Surfactant Vesicles in Templating Approaches,* Ph.D. Thesis, Eindhoven University of Technology **1999**.
[15] M. Jung, D. H. W. Hubert, A. M. van Herk, A. L. German, *Macromol. Symp.*, in press.
[16] R. G. Laughlin, R. L. Munyon, J. L. Burns, T. W. Coffindaffer, Y. Talmon, *J. Phys. Chem.* **1992**, *96*, 374.
[17] The phase transition temperatures of DMPC at pH 7 are: T_m = 14.3 °C for $L_\beta' \rightarrow P_\beta'$, and T_m = 23.9 °C for $P_\beta' \rightarrow L_\alpha$. See *Phospholipids Handbook* (Ed: G. Cevc), Marcel Dekker, New York **1993**.
[18] The area compressibility modulus, K, of DMPC in the L_β phase is K = 855 mN/m and in the L_α phase is K = 145 mN/m. The bending stiffness, κ, is expected to decrease at the same ratio; see E. Sackmann, in *Structure and Dynamics of Membranes* (Eds: E. Sackmann, R. Lipowsky), Elsevier/North-Holland, Amsterdam **1995**, Ch. 5.
[19] P. M. Frederik, M. C. A. Stuart, P. H. H. Bomans, W. M. Busing, K. N. H. Burger, A. J. Verkleij, *J. Microsc.* **1991**, *161*, 253.

Phase Separation of Carbon Nanotubes and Turbostratic Graphite Using a Functional Organic Polymer**

By *Jonathan N. Coleman*, *Alan B. Dalton*, *Seamus Curran*, *Angel Rubio*, *Andrew P. Davey*, *Anna Drury*, *Brendan McCarthy*, *Bernd Lahr*, *Pulickel M. Ajayan*, *Siegmar Roth*, *Robert C. Barklie*, and *Werner J. Blau**

Since their discovery in the early nineties,[1] carbon nanotubes in their various forms have generated much interest. Attention has been focused on the unusual electronic[2,3] and mechanical[4,5] properties predicted for these materials. Carbon nanotubes occur in two distinct forms, single-walled nanotubes (SWNT), which are composed of a graphene sheet rolled into a cylinder and multi-walled nanotubes (MWNT), which consist of multiple concentric graphene cylinders. The electronic properties of nanotubes depend on how the hexagonal carbon lattice is rolled up i.e. their chirality. Individual single walled tubes can be metallic or semiconducting, depending on their chirality and diameter.

Nanotubes are expected to have many potential applications, but their nature makes them difficult to purify and process. This is because the powder produced using production methods such as arc discharge is actually a multiphase system containing nanotubes, carbon anions, and turbostratic graphite. To date the best reported yields of MWNT are in the region of 20–30 %. While there are established purification methods such as oxidation, these tend to be extremely wasteful, generally giving less than one percent yield. We suggest that the solution to this problem is to incorporate nanotubes into a polymer matrix that acts as a filtration system. Recently we have reported some of these interesting properties when composite structures are formed from nanotubes and a conjugated polymer, poly(*m*-phenylene-*co*-2,5-dioctoxy-*p*-phenylenevinylene) (PmPV, Fig. 1a).[6,7]

To prepare the composite, multi-walled nanotubes produced in a Krätschmer generator[8] were added to a solu-

[*] Prof. W. J. Blau, Dr. J. N. Coleman, Dr. A. B. Dalton, Dr. S. Curran, Dr. A. P. Davey, A. Drury, B. McCarthy, B. Lahr, Dr. R. C. Barklie
Department of Physics, University of Dublin
Trinity College, Dublin 2 (Republic of Ireland)
Dr. S. Roth
Max Planck Institut für Festkörperforschung
Heisenberg Str. 1, Stuttgart, D-70569 (Germany)
Prof. A. Rubio
Departamento Fisica Teorica
Universidad de Valladolid, E-47011 Valladolid (Spain)
Prof. P. M. Ajayan
Department of Materials Science and Engineering
Rensseler Polytechnic Institute, Troy, NY 12180-3590 (USA)

[**] This work was supported by the European Union through TMR Contract No. Namitech, EBRFMRX-CT96-0067(DG12-MIHT). AR acknowledges financial support for JCyL (Grant VA28/99). We thank Mr. James Egan for helpful discussions.

  0935-9648/00/0302-0213 $ 17.50+.50/0

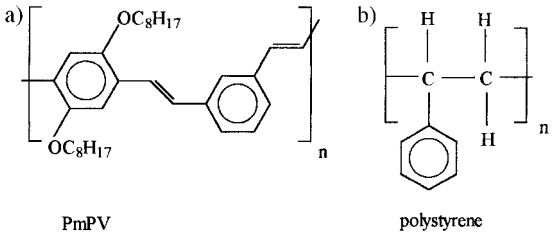

Fig. 1. Repeat unit structure of the polymers, poly(*m*-phenylene-*co*-2,5-dioctoxy-*p*-phenylenevinylene) and polystyrene.

tion of the polymer in toluene. The suspension was sonicated for 30 min in a low power (60 W) sonic bath then allowed to settle for 3 days. The suspension was then decanted from the settled solid. This suspension is stable over indefinite periods; no subsequent settling of material has been observed over periods of months. The suspended material was drop-cast onto carbon grids and examined using transmission electron microscopy (TEM).

A transmission electron micrograph of the edge of composite film is shown in Figure 2a. It is clear from this picture that there is virtually no carbonaceous material other than nanotubes present. In addition to this, the nanotubes appear well dispersed in the film. There is a relatively strong interaction between polymer and nanotube as the polymer is seen to wet all the nanotubes in the figure.

Fig. 2. A TEM micrograph of nanotubes protruding from the edge of a composite film.

In order to investigate the purity of the extracted material, Raman spectroscopy was employed to examine the spectroscopic properties of nanotube powder compared to a composite thin film. The MWNT powder spectrum is shown in Figure 3a. The excitation wavelength was 514 nm. The broad feature at 1350 cm^{-1} is typical of unpurified nanotube samples and arises from amorphous graphite carbon particles and defect sites on nanotubes. The peak at 1581 cm^{-1} is assigned to the E_{2g} mode of the multi-wall nanotubes, similar to that found for highly organized pyrolitic graphite. The Raman spectrum of a composite thin film is shown in Figure 3b. The dominant feature centered at 1581 cm^{-1} is due to the nanotubes. An indication of the proportion of nanotubes to amorphous material is given by the ratio of the intensities of the 1581 cm^{-1} relative to the 1350 cm^{-1}. The comparison of Figure 3a and 3b demonstrates a higher proportion of nanotubes to amorphous material in the composite sample. We suggest that in the preparation process, the vast majority of amorphous material settles to the bottom leaving nanotubes suspended in the polymer solution. Decanting thus separates suspended nanotubes from the amorphous material. In this case, the binding of the polymer to the nanotubes displaces amorphous material from the nanotube surfaces, keeping the majority of the nanotubes in the polymer solution whilst removing excess carbonaceous materials.

In order to test this hypothesis solutions of polymer and nanotube material were prepared as before (10 % mass fraction nanotubes, 20 mg/mL solvent). The nanotubes were sonicated in the presence of PmPV and toluene and allowed to settle for 7 days. However, instead of decanting off the suspension the solution was carefully separated into three fractions, the top, middle, and bottom part. These fractions were then drop cast onto spin free glass plates for electron paramagnetic resonance (EPR) analysis. This technique measures the absorption of microwaves by a sample in the presence of a magnetic field. Transitions are induced between the $m_s = 1/2$ and $m_s = -1/2$ spin states of any unpaired electrons in the sample. Information about the environment of the electron can be deduced from the position and shape of the absorption line. For technical reasons the first derivative of the line-shape is usually reported.

EPR studies have been carried out on various nanotube materials by several groups.[9,10] It is generally accepted that the signature at room temperature, of an unpaired electron on a MWNT has the following characteristics. The line-shape of the microwave absorption is Lorentzian, with a width of approximately 10 G (10^{-3} T) and the g_0 value (a quantity that describes the position of the absorption) is close to 2.01. Conversely, for an unpaired electron associated with turbostratic graphite the line width is generally in excess of 15 G and $g \geq 2.02$. As these lines are well separated it is possible to deconvolute them.

The spectra obtained from these fractions are shown in Figure 4. In these graphs, the EPR spectra of the first two fractions (top and middle) are highly symmetrical. This indicates that microwaves are being absorbed by one spin system only. Thus, what was originally a two-phase system (fullerenes and turbostratic graphite), is now a single-phase system. In this description we are neglecting the polymer phase as it has an almost negligable microwave absorption. The only indication we see of the polymer's EPR signal is the small high field shoulder. As we can see from Table 1 both the *g* values and widths of this line agree well with the predicted values of $g = 2.01$ and $\Delta B = 10$ G for multi-walled

  0935-9648/00/0302-0214 $ 17.50+.50/0

ADVANCED MATERIALS

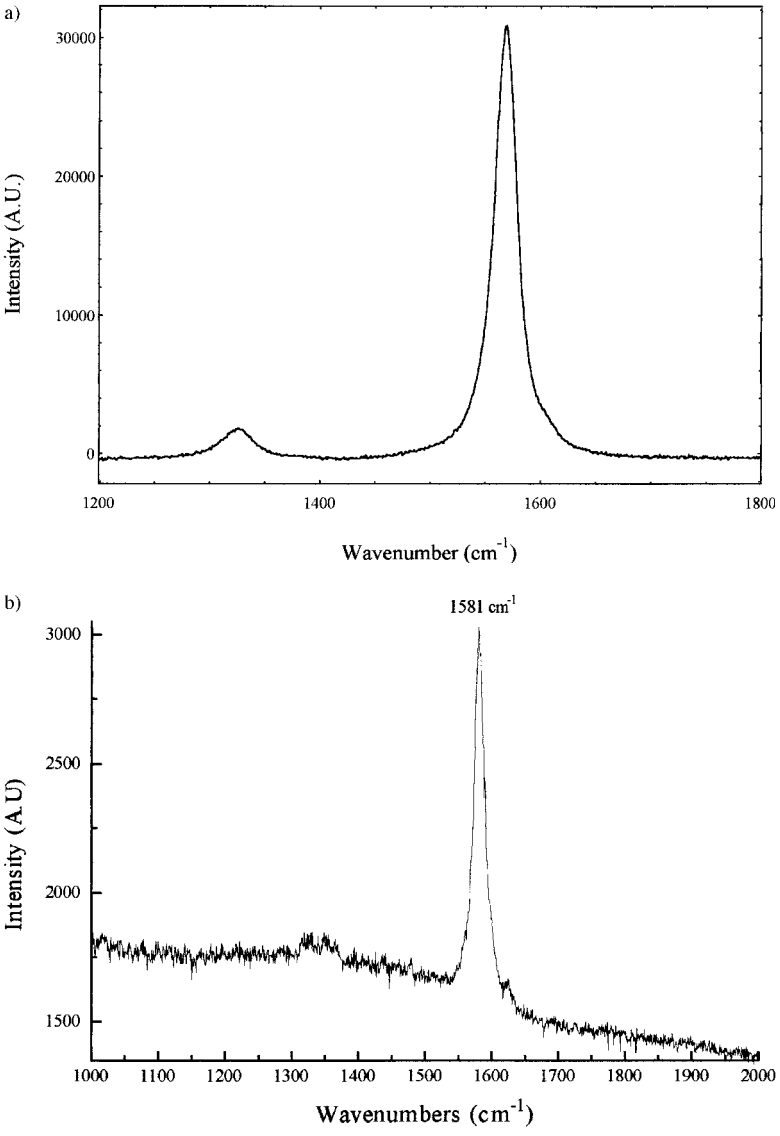

Fig. 3. a) Raman spectrum of multi-walled nanotube powder produced in the arc generator using the laser line at 514 nm. b) Raman spectrum of the composite material. The laser line used is at 514 nm.

Table 1. A summary of the results of Figure 3, The g values, linewidths, and signal intensities for three different composites, for top, middle, and bottom fractions. Fraction 1 refers to the top fraction. The results in the fraction 3 rows are parameters gained from two line fits to the spectra.

Fraction	g	ΔB [G]	Signal intensity [au]
PmPV Fr 1	2.0106	10.9	2.12
PmPV Fr 2	2.0111	10.4	3.09
PmPV Fr 3	2.0102	8.9	4.53
	2.0192	24.9	69.57

nanotubes. This shows that while nanotubes are being held in solution by the host material, all of the turbostratic graphite precipitates out.

This can clearly be seen in the spectra of the third (bottom) fraction. It is apparent that the major proportion of these spectra is due to a line with $g \sim 2.02$ and $\Delta B \sim 25$ G. This, as we have seen, is clearly due to turbostratic graphite. In addition to this however there is a significant nanotube component as expected because nanotubes should be more or less evenly distributed throughout the original solution. It is clear however that the nanotube component in the third fraction seems large in comparison to the spectrum of the nanotube powder. This can be explained as follows. Before film preparation each fraction was sonicated in order to homogenize it. However, the larger fragments of turbostratic graphite tend to settle very quickly and so it is extremely difficult to cast a film containing the exact composition of the final fraction. Thus, the signal intensity values quoted for the third fractions cannot be considered exact and should be used only as rough guides.

In order to show that this is not just a viscosity or a buoyancy effect, the procedure was repeated using polystyrene as the host. The EPR spectra of the top and bottom fractions are shown in Figure 5. In the case of this material, it was immediately clear visually that both nanotubes and turbostratic graphite had precipitated completely after only a few hours. In the spectra due to the polystyrene composite, the first fraction exhibited only one line of g = 2.0035 and width 7.7 G. This line is due to polystyrene, indicating that virtually no nanotubes were held in solution. The bottom fraction was similar to that in Figure 4 with components of g = 2.0101 and 2.0184 and widths 10.5 G and 23 G representing nanotubes and turbostratic graphite, respectively.

Solutions of a semi-conjugated organic polymer have been shown to be capable of suspending nanotubes indefinitely whilst the accompanying amorphous graphite settles out. In the case of a non-conjugated polymer such as polystyrene, this was not observed and all the carbonaceous material settled out. We have demonstrated using both Raman spectroscopy and electron paramagnetic resonance that it is possible to purify nanotubes using certain polymers as extracting agents.

Received: May 27, 1999
Final version: November 2, 1999

  0935-9648/00/0302-0215 $ 17.50+.50/0

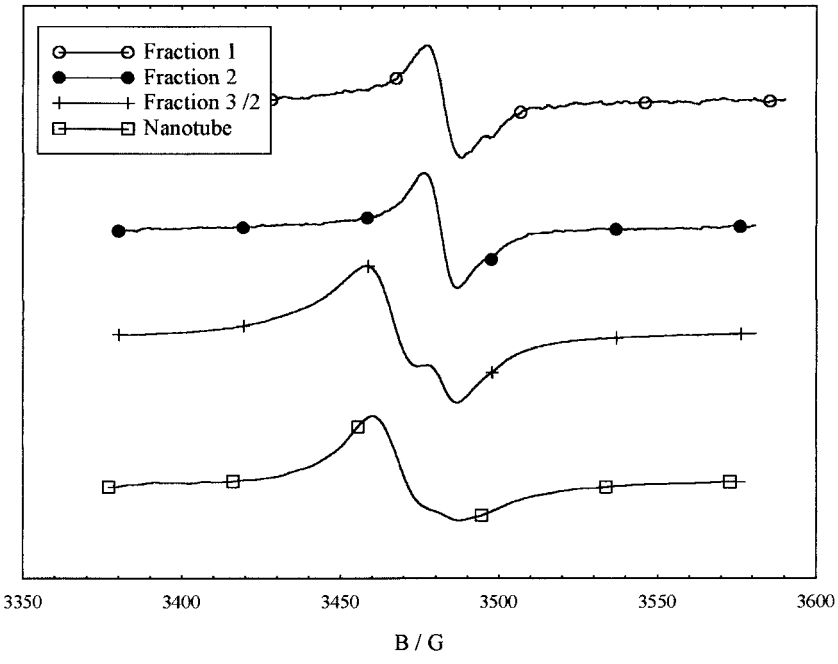

Fig. 4. EPR spectra of films made from fractions taken from a 10 % mass fraction PmPV-MWNT solution. Fraction 1 refers to the fraction taken from the top of the solution while fraction 3 refers to the fraction taken from the bottom of the solution. The nanotube powder EPR spectrum is shown for comparison. Note that the fraction 3 spectrum has been scaled down by a factor of two for clarity.

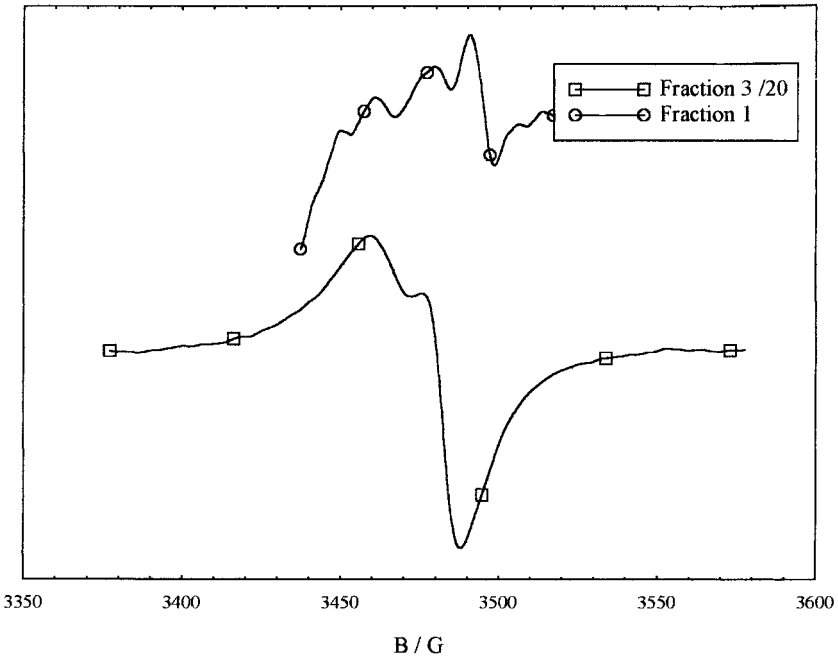

Fig. 5. Top and bottom fractions taken from a polystyrene-MWNT composite. The spectrum in the top fraction is due to polystyrene. No nanotubes were observed in any but the bottom fraction. Note, fraction 3 has been scaled down by a factor of 20 for clarity.

[1] S. Iijima, *Nature* **1991**, *354*, 56.
[2] M. S. Dresselhaus, G. Dresselhaus, P. C. Eklund, *Science of Fullerenes and Carbon Nanotubes*, Academic Press, San Diego, CA **1996**.
[3] Special issue on nanotubes, *Carbon* **1996**, *33*.
[4] M. M. J. Treacy, T. W. Ebbesen, J. M. Gibson, *Nature* **1996**, *381*, 678.
[5] E. Hernandez, C. Goze, P. Bernier, A. Rubio, *Phys. Rev. Lett.* **1998**, *80*, 4502.
[6] S. Curran, P. M. Ajayan, W. Blau, D. L. Carroll, J. N. Coleman, A. B. Dalton, A. P. Davey, A. Drury, B. McCarthy, S. Maier, A. Strevens, *Adv. Mater.* **1998**, *10*, 1091.
[7] J. N. Coleman, S. Curran, A. B. Dalton, A. P. Davey, B. McCarthy, W. Blau, R. C. Barklie, *Phys. Rev. B* **1998**, *58*, 7492.
[8] W. Krätschmer, L. D. Lamb, K. Fostiropoulos, D. R. Huffman, *Nature* **1990**, *347*, 354.
[9] O. Chauvet, L. Forro, W. Basca, D. Ugarte, B. Doudin, W. de Heer, *Phys. Rev. B* **1995**, *52*, 6963.
[10] S. J. Bandow, *Appl. Phys.* **1996**, *80*, 1029.

  0935-9648/00/0302-0216 $ 17.50+.50/0